© 2022. Published by The Company of Biologists Ltd | Development (2022) 149, dev200456. doi:10.1242/dev.200456

RESEARCH REPORT

Distinct contributions of ECM proteins to basement membrane mechanical properties in *Drosophila*

Uwe Töpfer[1], Karla Yanín Guerra Santillán[1,2,3], Elisabeth Fischer-Friedrich[2,3] and Christian Dahmann[1,3,*]

ABSTRACT

The basement membrane is a specialized extracellular matrix (ECM) that is crucial for the development of epithelial tissues and organs. In *Drosophila*, the mechanical properties of the basement membrane play an important role in the proper elongation of the developing egg chamber; however, the molecular mechanisms contributing to basement membrane mechanical properties are not fully understood. Here, we systematically analyze the contributions of individual ECM components towards the molecular composition and mechanical properties of the basement membrane underlying the follicle epithelium of *Drosophila* egg chambers. We find that the Laminin and Collagen IV networks largely persist in the absence of the other components. Moreover, we show that Perlecan and Collagen IV, but not Laminin or Nidogen, contribute greatly towards egg chamber elongation. Similarly, Perlecan and Collagen, but not Laminin or Nidogen, contribute towards the resistance of egg chambers against osmotic stress. Finally, using atomic force microscopy we show that basement membrane stiffness mainly depends on Collagen IV. Our analysis reveals how single ECM components contribute to the mechanical properties of the basement membrane controlling tissue and organ shape.

KEY WORDS: *Drosophila*, Egg chamber, Basement membrane, Collagen, Laminin, Nidogen, Perlecan, Atomic force microscopy

INTRODUCTION

The shaping of epithelial tissues during animal development depends on the generation of mechanical force and compliance of cells towards mechanical stress. Compliance towards stress is influenced by cell mechanical properties determined by the actomyosin network structure, Myosin motor protein activity and the underlying basement membrane (Khalilgharibi and Mao, 2021; Molnar and Labouesse, 2021). Basement membranes, specialized extracellular matrices (ECMs) that provide mechanical support to epithelia, promote cell survival, cell polarization and cell differentiation, serve as a substrate for cell migration, and are important for shaping epithelia during animal development (Jayadev and Sherwood, 2017; Sekiguchi and Yamada, 2018; Walma and Yamada, 2020). Basement membranes influence epithelial shape based on their mechanical properties (Khalilgharibi and Mao, 2021). Basement membranes are typically composed of four main components: Laminin, Collagen IV, Nidogen and Perlecan (Pozzi et al., 2017; Sekiguchi and Yamada, 2018). Laminins, a large family of heterotrimeric (α,β,γ) glycoproteins, self-assemble into networks linked via integrins and dystroglycans to the cell plasma membrane (Yamada and Sekiguchi, 2015). Collagen IV has a triple-stranded helical structure forming networks by covalent interactions strengthened through their terminal domains (Wu and Ge, 2019). Laminin and Collagen IV interact with the glycoprotein Nidogen and the proteoglycan Perlecan to form a highly interconnected molecular meshwork (Pozzi et al., 2017; Sekiguchi and Yamada, 2018). The *de novo* basement membrane assembly is hierarchical, beginning with Laminin, followed by the addition of Collagen IV (Matsubayashi et al., 2017; Pöschl et al., 2004). To what extent the presence of these main components is interdependent during the maintenance of basement membranes and to what extent individual components contribute to mechanical properties of basement membranes is not well understood.

The *Drosophila* egg chamber is a useful model system to investigate how individual ECM components contribute to mechanical properties of basement membranes (Isabella and Horne-Badovinac, 2015a; Khalilgharibi and Mao, 2021). In contrast to vertebrates, the *Drosophila* genome comprises a simple set of genes encoding the main basement membrane components: four genes (*LanA*, *wing blister*, *LanB1*, *LanB2*) encode Laminin subunits, the two α1-chains and one α2-chain forming the Collagen IV triple helical structure are encoded by *ColIVα1* (also known as *Col4a1*) and *ColIVα2* (*viking*), and Nidogen and Perlecan are encoded by single genes, *Ndg* and *Pcan* (*terribly reduced optic lobes*), respectively (Fig. 1A) (Hynes and Zhao, 2000). Egg chambers are composed of germline cells surrounded by a single-cell-layered somatic follicle epithelium, assemble in the germarium and mature through 14 stages to give rise to eggs (Fig. 1B) (Spradling, 1993). During maturation, egg chambers increase volume ∼1000-fold and change shape from spherical to ellipsoid (elongated). Follicle cells migrate as a collective on their underlying basement membrane in a direction perpendicular to the anteroposterior axis of egg chambers. Collective follicle cell migration results in egg chamber rotation and the orientation of basement membrane fibers parallel to the migration direction (Haigo and Bilder, 2011). Oriented basement membrane fibers, in conjunction with parallel oriented intracellular actin stress fibers, build a ‘molecular corset’ that contributes to egg chamber elongation (Bateman et al., 2001; Conder et al., 2007; Frydman and Spradling, 2001; Gutzeit et al., 1991; Haigo and Bilder, 2011; Horne-Badovinac et al., 2012; Lerner et al., 2013; Lewellyn et al., 2013; Viktorinová and Dahmann, 2013; Viktorinová et al., 2009). Atomic force microscopy (AFM) measurements have shown that the stiffness of the basement membrane increases during stages 3-8 and that basement membrane is stiffer in the central region of egg chambers compared with the

[1]Institute of Genetics, Technische Universität Dresden, 01062 Dresden, Germany. [2]Biotechnology Center, Technische Universität Dresden, 01307 Dresden, Germany. [3]Cluster of Excellence Physics of Life, Technische Universität Dresden, 01062 Dresden, Germany.

*Author for correspondence (christian.dahmann@tu-dresden.de)

C.D., 0000-0001-6822-0964

Handling Editor: Thomas Lecuit
Received 10 December 2021; Accepted 21 April 2022

Development (2022) 149, dev200456. doi:10.1242/dev.200456

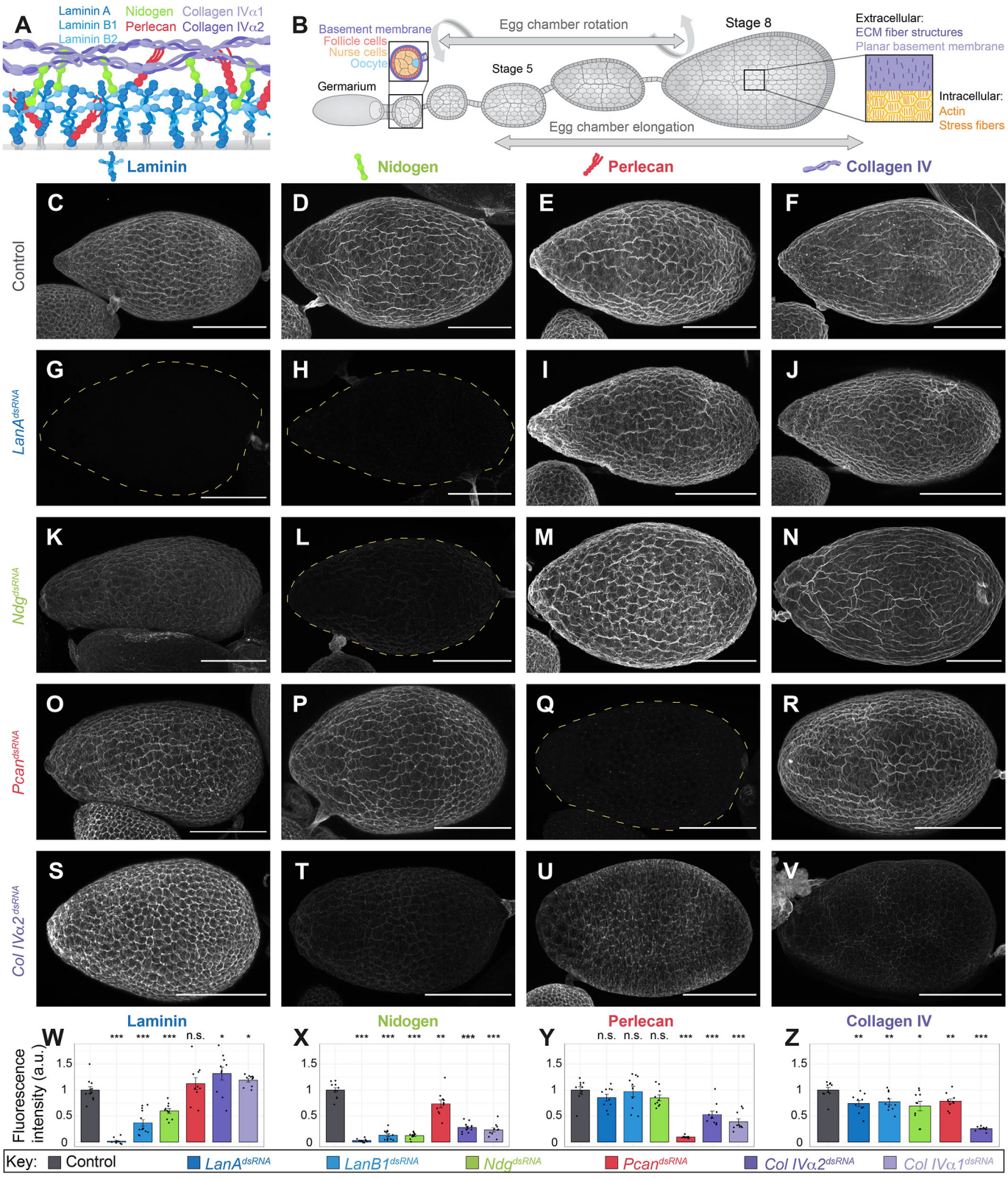

Fig. 1. Interdependence of basement membrane components. (A) Schematic of basement membrane composition. (B) Schematic of egg chamber development. (C-V) Antibody stainings detecting the indicated proteins of stage 8 egg chambers expressing no *UAS*-transgene (control) or the indicated transgenes under *GR1-Gal4*. Dashed lines indicate outlines of egg chambers. (W-Z) Mean fluorescence intensity, normalized to controls, of the indicated antibody stainings of stage 8 egg chambers expressing no *UAS*-transgene (control) or the indicated transgene (key) under *GR1-Gal4*. In Z, only the *ColIVα2*^{dsRNA}, not the *ColIVα1*^{dsRNA}, transgene was used. *n*>9 egg chambers per genotype and staining. Mean±s.e.m. are shown. **P*<0.01, ***P*<0.005, ****P*<0.001 (Welsh two-sided *t*-test). Black dots show individual measurements. n.s., not significant. Scale bars: 50 µm.

Development (2022) 149, dev200456. doi:10.1242/dev.200456

poles at stage 8 (Chlasta et al., 2017; Crest et al., 2017; Díaz de la Loza et al., 2017). Basement membrane stiffness depends on Collagen IV (Chlasta et al., 2017; Crest et al., 2017). Mutants of Collagen IV fail in egg chamber elongation (Haigo and Bilder, 2011), indicating that basement membrane stiffness is important for reshaping egg chambers.

Here, we report a systematic analysis of interdependencies of the four ECM components Laminin, Nidogen, Perlecan and Collagen IV and their individual contributions to basement membrane mechanical properties. We show that Laminin and Collagen IV networks can persist partially independently of each other. Moreover, Laminin has a minor contribution and Collagen IV has a major contribution to basement membrane mechanical properties, thus revealing distinct contributions of ECM components to basement membrane mechanical properties.

RESULTS AND DISCUSSION

Laminin and Collagen IV networks persist partially independently

The basement membrane is a highly complex network in which single components interact with multiple binding partners (Naba et al., 2012; Randles et al., 2017). To test whether level and subcellular localization of different basement membrane proteins is interdependent, we used RNA interference to knock down expression of either *LanA*, *LanB1*, *Ndg*, *Pcan*, *ColIVα1* or *ColIVα2* in *Drosophila* follicle cells from stage 3 onwards using the *GR1-Gal4* driver line (Tran and Berg, 2003) (Fig. S1A,A′) (Laminin A is the only α-subunit expressed in these cells; Schneider et al., 2006). Protein expression and localization were quantified by staining with antibodies against Laminin, Nidogen, Perlecan or a GFP antibody against ColIVα2::GFP expressed from an exon trap line (Buszczak et al., 2007). Compared with controls (Fig. 1C-F), levels of the targeted proteins were significantly decreased from stage 6 through at least stage 10 (Fig. 1C-G,L,Q,V-Z; Fig. S2A-Z), indicating that the knockdowns were efficient. Protein expression levels and localizations were analyzed in detail at stage 8. Laminin protein level decreased (reduction of staining intensity by ∼40%) in *Ndg* knockdown (Fig. 1K,W), was unaffected in *Pcan* knockdown (Fig. 1O,W) and was slightly increased (by ∼20-30%) in *ColIVα1* or *ColIVα2* knockdowns (Fig. 1S,W), the latter indicating a compensatory increase in Laminin when Collagen IV levels are reduced. Furthermore, Nidogen protein level strongly decreased in Laminin or Collagen IV knockdowns (by ∼91% and ∼75%, respectively) (Fig. 1H,T,X) and only slightly decreased (by ∼26%) in *Pcan* knockdown (Fig. 1P,X). Moreover, Perlecan protein level was only affected in Collagen IV knockdowns (Fig. 1I,M,U,Y), where it decreased (by ∼47% and ∼61%), consistent with observations in *Drosophila* embryo (Hollfelder et al., 2014), wing imaginal disc (Pastor-Pareja and Xu, 2011), fat body (Dai et al., 2018) and egg chamber (Haigo and Bilder, 2011; Isabella and Horne-Badovinac, 2015b) basement membranes. Finally, Collagen IVα2-GFP-protein level slightly decreased (by ∼21-31%) in each of the knockdowns (Fig. 1J,N,R,Z). Subcellular localizations of Collagen IV and Nidogen were not detectably altered in knockdowns of other basement membrane proteins (Fig. S3A,C-C″,E-E″,G-G″,I-I″,K-K″,M-M″,O-O″,Q-Q″,S-S″,U-U″).

Subcellular localization of Perlecan was also unchanged in Laminin or *Ndg* knockdowns (Fig. S3D-D″,H-H″,L-L″,P-P″). Interestingly, Perlecan mislocalized to lateral cell membranes, in particular at tricellular vertices, in Collagen IV knockdowns (Fig. S3T-T″). Similarly, Laminin mislocalized to lateral cell membranes in Collagen IV knockdowns (Fig. S3B-B″,F-F″,R-R″'), but also in *Pcan* knockdown (Fig. S3N-N″). Laminin localization was unaffected in the *Ndg* knockdown (Fig. S3J-J″).

Our analyses of protein levels and subcellular localizations after knockdown lead us to the following conclusions. First, the presence of Nidogen depends on both Laminin and Collagen IV, consistent with its role as a protein linking the Laminin and Collagen IV networks (Dai et al., 2018, and references therein). A dependency of Nidogen on Laminin has been previously shown in the *Drosophila* embryo (Hollfelder et al., 2014; Wolfstetter and Holz, 2012). Second, the presence of Laminin, and to a lesser extent of Collagen IV, requires Nidogen, showing a mutual interdependency between Nidogen and Laminin proteins. Third, the Laminin network is maintained largely independently from Collagen IV, consistent with the Laminin network being directly bound by integrins to the basal cell surface (Yamada and Sekiguchi, 2015). However, partial mislocalization of Laminin in Collagen IV or *Pcan* knockdowns indicates a role for Collagen IV and Perlecan in Laminin trafficking or retention. Fourth, localization and expression of Perlecan solely depend on Collagen IV, but not on Laminin or Nidogen. Fifth, although proper Collagen IV recruitment during the establishment of the basement membrane requires the Laminin network (Huang et al., 2003; Matsubayashi et al., 2017; Smyth et al., 1999; Urbano et al., 2009; Wolfstetter and Holz, 2012), our findings suggest that the maintenance of Collagen IV in the basement membrane does not strongly depend on the Laminin network.

Perlecan and Collagen IV make a major contribution to egg chamber elongation

We next sought to analyze individual contributions of Laminin, Nidogen, Perlecan and Collagen IV with respect to mechanical properties of the basement membrane. Egg chamber elongation depends on basement membrane mechanical properties (Chen et al., 2019; Chlasta et al., 2017; Crest et al., 2017; Díaz de la Loza et al., 2017; Haigo and Bilder, 2011), providing a functional assay. We knocked down *LanA*, *Ndg*, *Pcan* or *ColIVα2* expression in follicle cells and quantified egg chamber elongation by calculating the length ratio of the long-to-short axis of stage 2-14 egg chambers (aspect ratio, Fig. 2C). Compared with controls (Fig. 2A,B), knockdowns of *LanA* or *Ndg* had no obvious effect on egg chamber elongation except for at stage 8 (Fig. 2D-I). At this stage, *LanA* knockdown resulted in an increased aspect ratio that correlated with an unusually pointed anterior end of the egg chamber (Fig. 2D,F). Decreased *LanA* activity already induced in the germarium results in hypo-elongated stage 14 egg chambers (Andersen and Horne-Badovinac, 2016; Frydman and Spradling, 2001), *Ndg* knockdowns had a decreased aspect ratio at stage 8 (Fig. 2I). Knockdown of *Pcan*, using two independent RNAi lines, resulted in a moderate decrease of egg chamber elongation from stage 8 onwards (Fig. 2J-L) (Isabella and Horne-Badovinac, 2015b). Egg chamber elongation was severely diminished from stage 8 onwards in *ColIVα2* knockdown (Fig. 2M-O) (Crest et al., 2017; Haigo and Bilder, 2011; Isabella and Horne-Badovinac, 2015b). Thus, Laminin and Nidogen have only a minor contribution to egg chamber elongation, whereas Collagen IV, and to a lesser extent Perlecan, are the major components of the basement membrane required for egg chamber elongation.

Egg chamber elongation, in part, depends on aligned basement membrane fibers, the orientation of which require egg chamber rotation (Haigo and Bilder, 2011). The velocity of egg chamber rotation at stage 8 was indistinguishable between controls and knockdowns of *LanA*, *Ndg* or *Pcan* (Fig. S4A-D,F), suggesting that the changes in basement membrane composition and mechanical

Development (2022) 149, dev200456. doi:10.1242/dev.200456

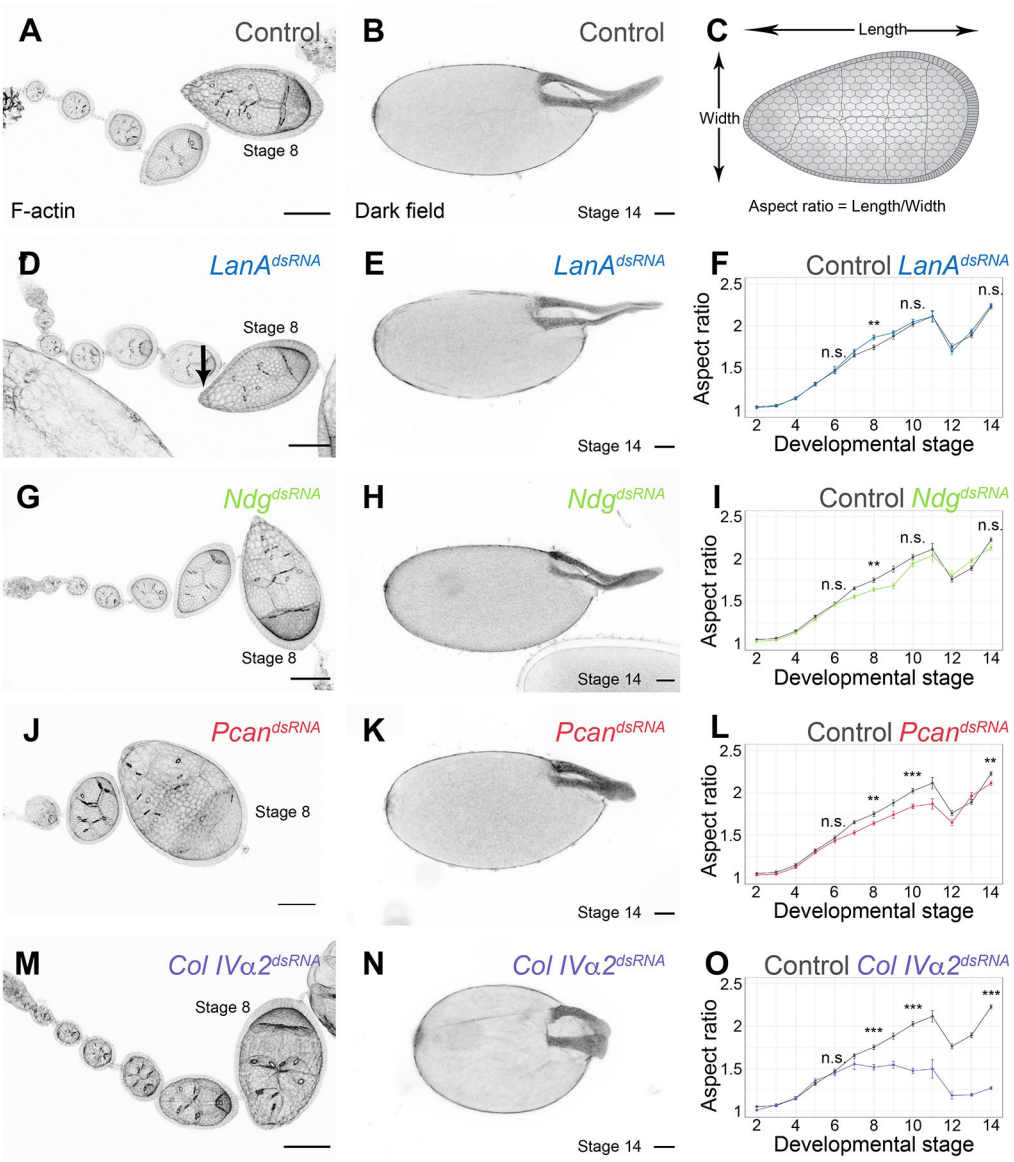

Fig. 2. Contributions of basement membrane components to egg chamber elongation. (A,D,G,J,M) F-actin stainings of egg chambers in ovarioles for knockdowns indicated. Arrow indicates pointed end of *LanA* knockdown egg chambers. (B,E,H,K,N) Dark-field images of stage 14 egg chambers for knockdowns indicated. Anterior to the left. (C) Schematic of aspect ratio measurements. (F,I,L,O) Aspect ratios of egg chambers as a function of developmental stage shown for control and knockdowns indicated. The same control data are used in F, I, L and O. $n>4$ egg chambers per stage and genotype. Mean±s.e.m. are shown. Welsh two-sided *t*-test was used to compare egg chambers of two different genotypes at a particular stage. $^{**}P<0.005$, $^{***}P<0.001$. n.s., not significant. Scale bars: 50 µm.

properties observed in these knockdowns cannot be accounted for by a lack of proper egg chamber rotation. Velocity was decreased in *ColIVα2* knockdown (Fig. S4E,F) (Haigo and Bilder, 2011). The greatly different contributions of Laminin and Nidogen versus Collagen IV to egg chamber elongation and rotation is consistent with our observation that Collagen IV protein levels are partially independent of Laminin and Nidogen (Fig. 1). Taken together, these results indicate that Laminin, Nidogen, Perlecan and Collagen IV make distinct contributions to basement membrane mechanical properties.

Perlecan and Collagen IV make a major contribution to resistance of egg chambers to osmotic stress

To further test the contribution of Laminin, Nidogen, Perlecan and Collagen IV to basement membrane mechanical properties, we knocked down their expression and analyzed the mechanical resistance of egg chambers to osmotic stress using an established assay (‘organ-swelling assay’) (Crest et al., 2017; Pastor-Pareja and Xu, 2011). Dissected egg chambers were placed in distilled water for 1 h, which led to their swelling and subsequent bursting (Fig. 3A). In general, the bursting of collagen networks is determined by the failure strain of the material, i.e. the amount of deformation at which the network breaks (Fig. 3B) (Roeder et al., 2002; Wang et al., 2002). In controls, ∼56% of egg chambers burst, with the egg chambers bursting on average after ∼12 min (Fig. 3C-E). Knockdown of *LanA* increased the fraction of burst egg chambers and slightly reduced the time span until the burst (Fig. 3C, D,F). *Ndg* knockdown behaved indistinguishably from controls (Fig. 3C,D,G). By contrast, all analyzed *Pcan* or *ColIVα2* knockdown egg chambers burst rapidly (Fig. 3C,D,H,I), as previously shown for Collagen IV knockdowns (Crest et al., 2017). Similarly, knockdown of *Pcan* leads to a rapid bursting of *Drosophila* wing imaginal discs upon osmotic stress (Pastor-Pareja and Xu, 2011). Thus, Nidogen and Laminin make no or a minor contribution, and Perlecan and Collagen IV make a major contribution, to the mechanical resistance of egg chambers to osmotic stress.

Collagen IV makes a major contribution to basement membrane stiffness

We finally analyzed the contribution of Laminin, Nidogen, Perlecan and Collagen IV to apparent basement membrane stiffness,

Development (2022) 149, dev200456. doi:10.1242/dev.200456

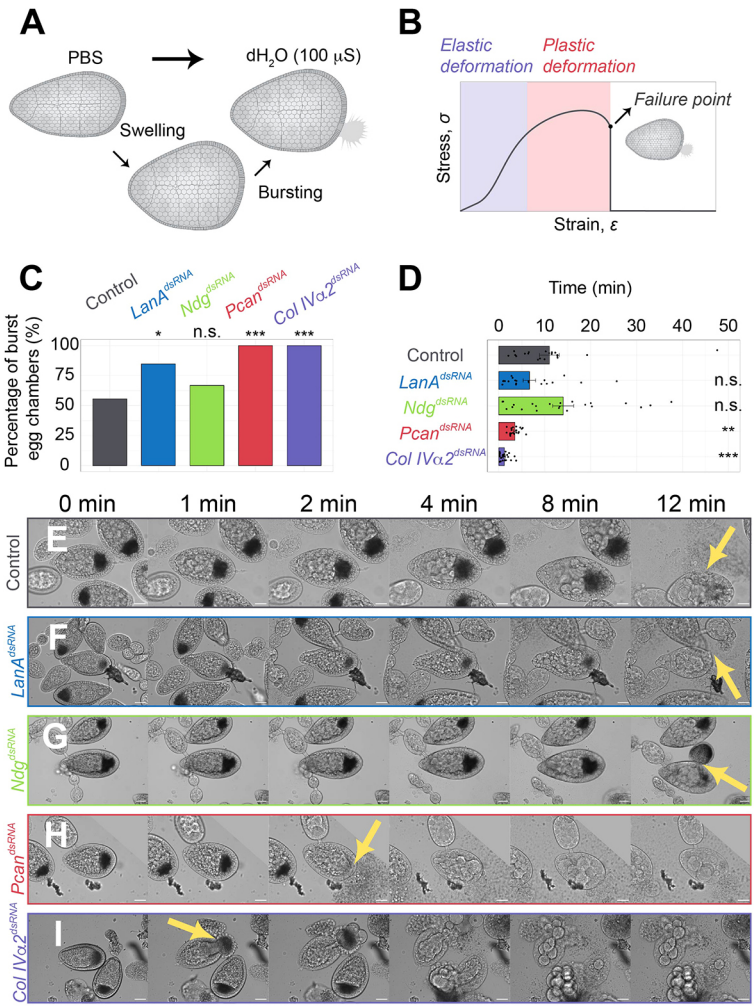

Fig. 3. Contributions of basement membrane components to resistance of egg chambers to osmotic stress. (A) Schematic of organ-swelling assay. (B) Schematic of a typical stress-strain curve for a collagen network with the material failure point indicated. (C) Ratio in percentage of burst to intact stage 8 egg chambers 1 h after addition of distilled water for control and knockdowns as indicated. $n>19$ analyzed egg chambers for each genotype. *$P<0.01$, ***$P<0.001$ (Chi-square test). (D) Time in distilled water until egg chambers burst. Mean±s.e.m. are shown. Black dots show individual measurements. **$P<0.005$, ***$P<0.001$ (Welsh two-sided *t*-test). (E-I) Time series of stage 8 egg chambers for control and knockdowns as indicated. Times after transfer to distilled water are shown. Yellow arrows indicate time points and sites of bursts. n.s., not significant. Scale bars: 50 µm.

anticipating a linear relationship between stress and strain (Fig. 4A). Stiffness (apparent Young's modulus) was probed by indentation with the cantilever tip of an atomic force microscope in the central or pole region of dissected stage 8 egg chambers (Fig. 4B,C). In controls, basement membrane stiffness was ∼60 kPa in the central (Fig. 4D,E) and ∼45 kPa in the pole region (Fig. 4F), consistent with previous measurements using indentation depth similar to those used in this work (Chen et al., 2019; Crest et al., 2017). Collagenase treatment of egg chambers decreased basement membrane material (Fig. S5) and strongly reduced basement membrane stiffness (Fig. 4D), demonstrating that the measured stiffness depends on basement membrane (Chlasta et al., 2017; Crest et al., 2017). Knockdown of *LanA* increased basement membrane stiffness in the central region (Fig. 4E) and decreased it in the pole region (Fig. 4F). This increased stiffness anisotropy (Fig. 4G) correlated with hyper-elongation of *LanA* knockdown egg chambers at stage 8 (Fig. 2D,F), consistent with the notion that stiffness anisotropy drives egg chamber elongation (Crest et al., 2017). *Ndg* knockdown resulted in a slightly decreased basement membrane stiffness in the central region (Fig. 4E), but did not affect the pole region (Fig. 4F). Knockdown of *Pcan* did not significantly alter basement membrane stiffness in either region (Fig. 4E,F) [we note that Chlasta et al. (2017), using a different AFM setup, reported a decreased basement membrane stiffness in *Pcan* knockdowns]. Finally, knockdown of *ColIVα2* strongly decreased basement membrane stiffness in both regions (Fig. 4E,F) (Chlasta et al., 2017; Crest et al., 2017). Thus, Collagen IV makes a major contribution to basement membrane stiffness in egg chambers.

In summary, we have used three different assays to investigate the contribution of individual ECM components to the mechanical properties of the basement membrane (Fig. 4H). Perlecan is important for egg chamber elongation and resistance to osmotic stress, but dispensable for basement membrane stiffness. Nidogen plays a minor role during egg chamber elongation and basement membrane stiffness, and is dispensable for the resistance to osmotic stress. Laminin plays a minor role during egg chamber elongation and resistance to osmotic stress and suppresses the stiffness anisotropy of the basement membrane. The differential requirements for Perlecan, Nidogen and Laminin indicate that the three assays reflect different functional aspects of the basement membrane in mechanically supporting the egg chamber. The organ-swelling assay interrogates in particular the mechanical properties of egg chambers at their poles, as suggested by frequent bursting at that location (Crest et al., 2017). Bursting frequency, however, does not correlate with basement membrane stiffness in pole regions. *Pcan* knockdown, for example, showed increased bursting frequency (Fig. 3C), yet basement membrane stiffness in the pole region was comparable with controls (Fig. 4F). The organ-swelling assay thus reflects the failure strain of the egg chamber material (see Fig. 3B) rather than basement membrane stiffness in the pole region. This is not surprising, as the failure strain and the stiffness often do not correlate positively (Bax et al., 2019; Haut, 1986; Leng et al.,

Development (2022) 149, dev200456. doi:10.1242/dev.200456

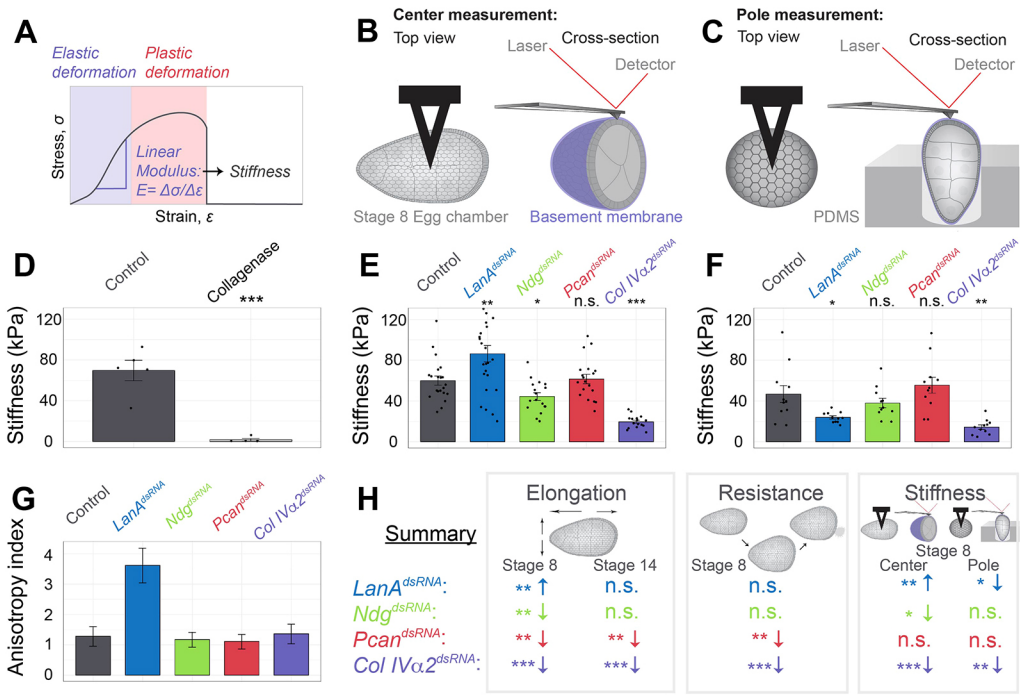

Fig. 4. Contributions of basement membrane components to basement membrane stiffness. (A) Schematic of typical stress-strain curve for a collagen network (linear relationship is used to calculate basement membrane stiffness as indicated). (B,C) Schematic of AFM measurements in the central (B) or in the posterior pole (C) region of stage 8 egg chambers. (D) Basement membrane stiffness (apparent Young's modulus) in the central region of egg chambers (*CollVα2::GFP; GR1-Gal4*) before (control) and after 1 h collagenase treatment is shown. *n*=5 egg chambers. Mean±s.e.m. are shown. ***P<0.001 (Welsh two-sided *t*-test). (E,F) Basement membrane stiffness (apparent Young's modulus) in the center (E) or in the posterior pole region (F) for control and knockdowns as indicated. *n*>15 egg chambers (central region); *n*=11 egg chambers (pole region). Mean±s.e.m. are shown. Black dots show individual measurements. *P<0.01, **P<0.005, ***P<0.001 (Welsh two-sided *t*-test). (G) Ratio of mean basement membrane stiffness in central and posterior pole region (anisotropy index) shown for control and knockdowns as indicated. Error bars show error propagation of the s.e.m. from central and pole regions (E,F). (H) Summary and comparison of the data shown in Figs 2-4. n.s., not significant.

2013). On the other hand, egg chamber elongation relies on the establishment of a stiffness gradient between the poles and the center of egg chambers (Chlasta et al., 2017; Crest et al., 2017). Finally, Collagen IV makes a major contribution to egg chamber elongation, resistance to osmotic stress and basement membrane stiffness. The greater contribution of the network-forming Collagen IV compared with Laminin towards conferring mechanical properties may reflect the ability of Collagen IV molecules to better resist mechanical stresses due to their covalent bonds, whereas laminins self-assemble only through weaker ionic interactions (Wu and Ge, 2019; Yamada and Sekiguchi, 2015).

Previous work has mainly analyzed mechanical properties of fibrillar collagens (including Collagen I) and other ECM components present, e.g. in connective tissues, ligaments or bones (reviewed by Sherman et al., 2015) and has shown that Collagen I, in contrast to laminins, bears tensile stresses. Similarly, our work suggests that in the basement membrane of *Drosophila* egg chambers Collagen IV mainly bears tensile stresses. The ability of Collagen I fibrils and higher order fibers to bear mechanical stress depends on multiple parameters, including fiber shape and orientation, mineralization and density of covalent cross-links (Sherman et al., 2015). Oriented fibril-like Collagen IV structures contribute to basement membrane stiffening of egg chambers (Chlasta et al., 2017), indicating that shape and orientation of fibril-like structures also determine mechanical properties of Collagen IV networks. Moreover, removal of bromide, an ion required for sulfilimine crosslinks of Collagen IV, from fly food results in hypo-elongated egg chambers (McCall et al., 2014), indicating that molecular cross-links further contribute to the ability of Collagen IV networks to bear mechanical stresses.

MATERIALS AND METHODS

Fly stocks and genetics

The fly stocks used were *GR1-Gal4* [Bloomington *Drosophila* Stock Center (BDSC), 36287], *UAS-mCD8::RFP* (BDSC, 32219), *UAS-LanA*^{dsRNA} (BDSC, 28071), *UAS-LanB1*^{dsRNA} (BDSC, 42616), *UAS-Ndg*^{dsRNA} (BDSC, 62902), *UAS-trol*^{dsRNA} (BDSC, 42783), *UAS-trol*^{dsRNA} [Vienna *Drosophila* Resource Center (VDRC), 110494], *UAS-Col4a1*^{dsRNA} (VDRC, 28369), *UAS-vkg*^{dsRNA} (BDSC, 50895), *vkg::GFP*^{G00454} [*Drosophila* Genetic Resource Center (DGRC), 110692] and *LanA::GFP* (VDRC, 318155). Flies were kept at 25°C on standard food. Crosses were raised at 18°C and virgin flies were transferred to 29°C for 2 days before dissection.

Immunohistochemistry

Ovaries from 2-day-old flies were dissected in PBS and fixed with 4% paraformaldehyde and 0.1% Triton X-100. The following primary antibodies were used: anti-Laminin (Gutzeit et al., 1991; 1:1000), anti-Nidogen (Wolfstetter et al., 2009; 1:500), anti-Perlecan (Friedrich et al., 2000; 1:1000), anti-GFP (Clontech, 632592, 1:2000) and anti-RFP (Chromotek, 5F8, 1:1000). The secondary antibodies used were goat anti-rabbit Alexa 488 (Molecular Probes, A27034, 1:200) and goat anti-rat Cy3 (Jackson ImmunoResearch, 112-165-167, 1:200). Rhodamin-Phalloidin (Thermo Fisher Scientific, R415, 1:200) was used to visualize F-actin. Images were acquired using a laser scanning microscope Zeiss LSM 880 or Zeiss LSM 980, or a microscope Zeiss Axio Observer Z1. Note that slight convolutions of the egg chamber surface (Fig. 1C-V) may be due to the long incubation time of fixation and permeabilization during the antibody staining.

Development (2022) 149, dev200456. doi:10.1242/dev.200456

Quantification of fluorescence intensity

Image stacks covering the entire apical-basal extent of follicle cells were acquired with the same laser intensity settings and were projected using the maximum projection method. Mean fluorescence intensity of *z*-projections was measured in corresponding regions of egg chambers using Fiji (Schindelin et al., 2012). To calculate the corrected mean fluorescence intensity, the mean fluorescence intensity value was reduced by the mean fluorescence intensity value of five egg chambers treated with secondary antibody only. For Fig. S3, image stacks were acquired in the central region of egg chambers and *x*-*z* images were then obtained by maximum projection of the orthogonal view using Fiji (Schindelin et al., 2012). For measurements of GFP fluorescence intensity during collagenase treatment, images were acquired every 2 min for 1 h.

Aspect ratio measurements

Egg chamber stages were determined as previously described (Jia et al., 2016; Spradling, 1993). Length and width of egg chambers were measured using Fiji (Schindelin et al., 2012).

Organ-swelling assay

The organ-swelling assay was performed as previously described (Crest et al., 2017) with the following exception: distilled water was set to a conductivity of 100 µS/cm^3.

Measurements of basement membrane stiffness using an atomic force microscope

Dissection of ovaries and measurements were performed in Schneider medium with supplements (Prasad et al., 2007). Basement membrane stiffness was measured using an atomic force microscope (Nanowizard I, JPK Instruments) mounted on a Zeiss Axiovert 200M wide-field microscope with a 20× objective (Zeiss, Plan Apochromat, NA=0.8) and a CCD camera (DMK 23U445, The Imaging Source). Standard pyramidal tips (MLCT-C, Bruker AFM probes) were used in all experiments. The nominal tip radius given by the manufacturer is 20 nm with a nominal spring constant of 0.01 N/m. Before each experiment, the actual cantilever spring constant was measured by means of thermal noise analysis (built-in software, JPK Instruments). Actual spring constant values ranged from 0.015-0.019 N/m. All measurements were performed in culture medium at room temperature.

For measurements in the central region, dissected egg chambers were placed into cell culture dishes (FluoroDish FD35-100) coated with poly-D-lysine. For measurements in the pole region, polydimethylsiloxane (PDMS) blocks with molds of diameter 120 µm and 140 µm and a depth of 100 µm were made [Center for Molecular and Cellular Bioengineering (CMCB) Microstructure Facility of the Technische Universität Dresden]. The PDMS block was mounted inside a cell culture dish and adhered to the glass bottom through gentle mechanical pressure. Then, the mounted PDMS block was plasma activated and coated with poly-D-lysine. Stage 8 egg chambers were manually isolated and transferred into the coated PDMS block (posterior to the top). Quick removal and addition of culture medium allowed adhesion of the egg chamber to the coated PDMS block.

AFM measurements were carried out in contact mode with the cantilever oriented approximately orthogonal to the egg chamber long axis (Fig. 4B, C). Each measurement consisted of 64 force curves acquired on a regular square lattice of 10×10 µm^2 placed in the central region or in the pole region of the egg chamber surface (Fig. 4B,C). Indentations were performed at an extension speed of 0.5 µm/s up to a maximal force of 0.4 nN. For each condition, at least five egg chambers were measured.

In order to extract basement membrane Young's moduli, force-indentation curves were fitted to the Hertz-Sneddon model (Sneddon, 1965) for a tip with a quadratic pyramid geometry and a half-angle to edge of 17.5°, assuming a Poisson ratio of 0.5. Fitting was performed using only the first 50 nm of indentation as reported earlier (Crest et al., 2017).

Egg chamber rotation

Egg chambers were dissected in egg chamber culture medium (Prasad et al., 2007) and adhered to glass bottom microwell dishes (MatTek) coated with poly-D-lysine. Egg chambers were imaged every minute for 20 min. *GR1-Gal4* driven expression of mCD8::RFP was used to visualize cell membranes. The distance of tricellular junction displacement after 20 min was measured by Fiji (Schindelin et al., 2012) and used to calculate the velocity of egg chamber rotation.

Collagenase treatment

Egg chambers were dissected in Schneider medium with supplements (Prasad et al., 2007). Dissected egg chambers were adhered to glass bottom microwell dishes (MatTek) coated with poly-D-lysine and were either treated with or without (control) 0.05% Collagenase I (Merck).

Statistical analysis

Statistical significance was calculated using the Welsh two-sided *t*-test or Chi-square test using R. To determine error propagation of the index of anisotropy, we used the standard formula for a ratio, i.e., if $f=\frac{x}{y}$, the propagation of the standard error of the mean is $\frac{s_f}{f}=\frac{s_x}{x}+\frac{s_y}{y}$. Where s_f, s_x and s_y are the standard error of the mean of the function, variable x and variable y, respectively.

Acknowledgements

We thank Stefan Baumgartner, Anne Holz, and Christoph von Bredow for providing antibodies, Klaus Reinhardt for access to the Zeiss LSM 880 microscope as well as the CMCB Light Microscopy Facility and the CMCB Microstructure Facility of the Technische Universität Dresden for their support. Stocks obtained from the BDSC (NIH P40OD018537), the VDRC and the DGRC were used in this study.

Competing interests

The authors declare no competing or financial interests.

Author contributions

Conceptualization: U.T., C.D.; Methodology: U.T., K.Y.G.S., E.F.-F.; Investigation: U.T., K.Y.G.S., E.F.-F.; Resources: C.D.; Writing - original draft: U.T., C.D.; Writing - review & editing: U.T., K.Y.G.S., E.F.-F., C.D.; Supervision: E.F.-F., C.D.; Project administration: C.D.; Funding acquisition: E.F.-F., C.D.

Funding

This work was supported by the Deutsche Forschungsgemeinschaft (DA586-16/2 to C.D.). E.F.-F. and C.D. were supported by the Deutsche Forschungsgemeinschaft under Germany's Excellence Strategy – EXC-2068-390729961 – Cluster of Excellence Physics of Life of TU Dresden. Open access funding provided by Technische Universität Dresden. Deposited in PMC for immediate release.

Peer review history

The peer review history is available online at https://journals.biologists.com/dev/article-lookup/doi/10.1242/dev.200456.

References

Andersen, D. and Horne-Badovinac, S. (2016). Influence of ovarian muscle contraction and oocyte growth on egg chamber elongation in *Drosophila*. *Development* **143**, 1375-1387. doi:10.1242/dev.131276

Bateman, J., Reddy, R. S., Saito, H. and Van Vactor, D. (2001). The receptor tyrosine phosphatase Dlar and integrins organize actin filaments in the *Drosophila* follicular epithelium. *Curr. Biol.* **11**, 1317-1327. doi:10.1016/S0960-9822(01)00420-1

Bax, D. V., Smalley, H. E., Farndale, R. W., Best, S. M. and Cameron, R. E. (2019). Cellular response to collagen-elastin composite materials. *Acta Biomater.* **86**, 158-170. doi:10.1016/j.actbio.2018.12.033

Buszczak, M., Paterno, S., Lighthouse, D., Bachman, J., Planck, J., Owen, S., Skora, A. D., Nystul, T. G., Ohlstein, B., Allen, A. et al. (2007). The Carnegie protein trap library: a versatile tool for *Drosophila* developmental studies. *Genetics* **175**, 1505-1531. doi:10.1534/genetics.106.065961

Chen, D. Y., Crest, J., Streichan, S. J. and Bilder, D. (2019). Extracellular matrix stiffness cues junctional remodeling for 3D tissue elongation. *Nat. Commun.* **10**, 3339. doi:10.1038/s41467-019-10874-x

Chlasta, J., Milani, P., Runel, G., Duteyrat, J. L., Arias, L., Lamire, L. A., Boudaoud, A. and Grammont, M. (2017). Variations in basement membrane mechanics are linked to epithelial morphogenesis. *Development* **144**, 4350-4362. doi:10.1242/dev.152652

Conder, R., Yu, H., Zahedi, B. and Harden, N. (2007). The serine/threonine kinase dPak is required for polarized assembly of F-actin bundles and apical-basal

polarity in the *Drosophila* follicular epithelium. *Dev. Biol.* **305**, 470-482. doi:10.1016/j.ydbio.2007.02.034

Crest, J., Diz-Muñoz, A., Chen, D.-Y., Fletcher, D. A. and Bilder, D. (2017). Organ sculpting by patterned extracellular matrix stiffness. *eLife* **6**, e24958. doi:10.7554/eLife.24958

Dai, J., Estrada, B., Jacobs, S., Sánchez-Sánchez, B. J., Tang, J., Ma, M., Magadán-Corpas, P., Pastor-Pareja, J. C. and Martín-Bermudo, M. D. (2018). Dissection of Nidogen function in *Drosophila* reveals tissue-specific mechanisms of basement membrane assembly. *PLoS Genet.* **14**, e1007483. doi:10.1371/journal.pgen.1007483

Díaz de la Loza, M. C., Díaz-Torres, A., Zurita, F., Rosales-Nieves, A. E., Moeendarbary, E., Franze, K., Martín-Bermudo, M. D. and González-Reyes, A. (2017). Laminin levels regulate tissue migration and anterior-posterior polarity during egg morphogenesis in *Drosophila*. *Cell Rep.* **20**, 211-223. doi:10.1016/j.celrep.2017.06.031

Friedrich, M. V., Schneider, M., Timpl, R. and Baumgartner, S. (2000). Perlecan domain V of *Drosophila melanogaster*. Sequence, recombinant analysis and tissue expression. *Eur. J. Biochem.* **267**, 3149-3159. doi:10.1046/j.1432-1327.2000.01337.x

Frydman, H. M. and Spradling, A. C. (2001). The receptor-like tyrosine phosphatase Lar is required for epithelial planar polarity and for axis determination within *Drosophila* ovarian follicles. *Development* **128**, 3209-3220. doi:10.1242/dev.128.16.3209

Gutzeit, H. O., Eberhardt, W. and Gratwohl, E. (1991). Laminin and basement membrane-associated microfilaments in wild-type and mutant *Drosophila* ovarian follicles. *J. Cell Sci.* **100**, 781-788. doi:10.1242/jcs.100.4.781

Haigo, S. L. and Bilder, D. (2011). Global tissue revolutions in a morphogenetic movement controlling elongation. *Science* **331**, 1071-1074. doi:10.1126/science.1199424

Haut, R. C. (1986). The influence of specimen length on the tensile failure properties of tendon collagen. *J. Biomech.* **19**, 951-955. doi:10.1016/0021-9290(86)90190-9

Hollfelder, D., Frasch, M. and Reim, I. (2014). Distinct functions of the Laminin beta LN domain and Collagen IV during cardiac extracellular matrix formation and stabilization of alary muscle attachments revealed by EMS mutagenesis in *Drosophila*. *BMC Dev. Biol.* **14**, 26. doi:10.1186/1471-213x-14-26

Horne-Badovinac, S., Hill, J., Gerlach, G., 2nd, Menegas, W. and Bilder, D. (2012). A screen for round egg mutants in *Drosophila* identifies *tricornered*, *furry*, and *misshapen* as regulators of egg chamber elongation. *G3* **2**, 371-378. doi:10.1534/g3.111.001677

Huang, C.-C., Hall, D. H., Hedgecock, E. M., Kao, G., Karantza, V., Vogel, B. E., Hutter, H., Chisholm, A. D., Yurchenco, P. D. and Wadsworth, W. G. (2003). Laminin alpha subunits and their role in *C. elegans* development. *Development* **130**, 3343-3358. doi:10.1242/dev.00481

Hynes, R. O. and Zhao, Q. (2000). The evolution of cell adhesion. *J. Cell Biol.* **150**, F89-F96. doi:10.1083/jcb.150.2.F89

Isabella, A. J. and Horne-Badovinac, S. (2015a). Building from the ground up: basement membranes in *Drosophila* development. *Curr. Top. Membr.* **76**, 305-336. doi:10.1016/bs.ctm.2015.07.001

Isabella, A. J. and Horne-Badovinac, S. (2015b). Dynamic regulation of basement membrane protein levels promotes egg chamber elongation in *Drosophila*. *Dev. Biol.* **406**, 212-221. doi:10.1016/j.ydbio.2015.08.018

Jayadev, R. and Sherwood, D. R. (2017). Basement membranes. *Curr. Biol.* **27**, R207-R211. doi:10.1016/j.cub.2017.02.006

Jia, D., Xu, Q., Xie, Q., Mio, W. and Deng, W. M. (2016). Automatic stage identification of *Drosophila* egg chamber based on DAPI images. *Sci. Rep.* **6**, 18850. doi:10.1038/Srep18850

Khalilgharibi, N. and Mao, Y. (2021). To form and function: on the role of basement membrane mechanics in tissue development, homeostasis and disease. *Open Biol.* **11**, 200360. doi:10.1098/rsob.200360

Leng, H., Reyes, M. J., Dong, X. N. and Wang, X. (2013). Effect of age on mechanical properties of the collagen phase in different orientations of human cortical bone. *Bone* **55**, 288-291. doi:10.1016/j.bone.2013.04.006

Lerner, D. W., McCoy, D., Isabella, A. J., Mahowald, A. P., Gerlach, G. F., Chaudhry, T. A. and Horne-Badovinac, S. (2013). A Rab10-dependent mechanism for polarized basement membrane secretion during organ morphogenesis. *Dev. Cell* **24**, 159-168. doi:10.1016/j.devcel.2012.12.005

Lewellyn, L., Cetera, M. and Horne-Badovinac, S. (2013). Misshapen decreases integrin levels to promote epithelial motility and planar polarity in *Drosophila*. *J. Cell Biol.* **200**, 721-729. doi:10.1083/jcb.201209129

Matsubayashi, Y., Louani, A., Dragu, A., Sánchez-Sánchez, B. J., Serna-Morales, E., Yolland, L., Gyoergy, A., Vizcay, G., Fleck, R. A., Heddleston, J. M. et al. (2017). A moving source of matrix components is essential for *de novo* basement membrane formation. *Curr. Biol.* **27**, 3526-3534.e4. doi:10.1016/j.cub.2017.10.001

McCall, A. S., Cummings, C. F., Bhave, G., Vanacore, R., Page-McCaw, A. and Hudson, B. G. (2014). Bromine is an essential trace element for assembly of Collagen IV scaffolds in tissue development and architecture. *Cell* **157**, 1380-1392. doi:10.1016/j.cell.2014.05.009

Molnar, K. and Labouesse, M. (2021). The plastic cell: mechanical deformation of cells and tissues. *Open Biol.* **11**, 210006. doi:10.1098/rsob.210006

Naba, A., Clauser, K. R., Hoersch, S., Liu, H., Carr, S. A. and Hynes, R. O. (2012). The matrisome: *in silico* definition and *in vivo* characterization by proteomics of normal and tumor extracellular matrices. *Mol. Cell. Proteomics* **11**, M111 014647. doi:10.1074/mcp.M111.014647

Pastor-Pareja, J. C. and Xu, T. (2011). Shaping cells and organs in *Drosophila* by opposing roles of fat body-secreted Collagen IV and Perlecan. *Dev. Cell* **21**, 245-256. doi:10.1016/j.devcel.2011.06.026

Pöschl, E., Schlötzer-Schrehardt, U., Brachvogel, B., Saito, K., Ninomiya, Y. and Mayer, U. (2004). Collagen IV is essential for basement membrane stability but dispensable for initiation of its assembly during early development. *Development* **131**, 1619-1628. doi:10.1242/dev.01037

Pozzi, A., Yurchenco, P. D. and Iozzo, R. V. (2017). The nature and biology of basement membranes. *Matrix Biol.*, **57-58**, 1-11.doi:10.1016/j.matbio.2016.12.009

Prasad, M., Jang, A. C.-C., Starz-Gaiano, M., Melani, M. and Montell, D. J. (2007). A protocol for culturing *Drosophila melanogaster* stage 9 egg chambers for live imaging. *Nat. Protoc.* **2**, 2467-2473. doi:10.1038/nprot.2007.363

Randles, M. J., Humphries, M. J. and Lennon, R. (2017). Proteomic definitions of basement membrane composition in health and disease. *Matrix Biol.* **57-58**, 12-28. doi:10.1016/j.matbio.2016.08.006

Roeder, B. A., Kokini, K., Sturgis, J. E., Robinson, J. P. and Voytik-Harbin, S. L. (2002). Tensile mechanical properties of three-dimensional type I Collagen extracellular matrices with varied microstructure. *J. Biomech. Eng.* **124**, 214-222. doi:10.1115/1.1449904

Schindelin, J., Arganda-Carreras, I., Frise, E., Kaynig, V., Longair, M., Pietzsch, T., Preibisch, S., Rueden, C., Saalfeld, S., Schmid, B. et al. (2012). Fiji: an open-source platform for biological-image analysis. *Nat. Methods* **9**, 676-682. doi:10.1038/nmeth.2019

Schneider, M., Khalil, A. A., Poulton, J., Castillejo-Lopez, C., Egger-Adam, D., Wodarz, A., Deng, W.-M. and Baumgartner, S. (2006). Perlecan and Dystroglycan act at the basal side of the *Drosophila* follicular epithelium to maintain epithelial organization. *Development* **133**, 3805-3815. doi:10.1242/dev.02549

Sekiguchi, R. and Yamada, K. M. (2018). Basement membranes in development and disease. *Curr. Top. Dev. Biol.* **130**, 143-191. doi:10.1016/bs.ctdb.2018.02.005

Sherman, V. R., Yang, W. and Meyers, M. A. (2015). The materials science of collagen. *J. Mech. Behav. Biomed. Mater.* **52**, 22-50. doi:10.1016/j.jmbbm.2015.05.023

Smyth, N., Vatansever, H. S., Murray, P., Meyer, M., Frie, C., Paulsson, M. and Edgar, D. (1999). Absence of basement membranes after targeting the *LAMC1* gene results in embryonic lethality due to failure of endoderm differentiation. *J. Cell Biol.* **144**, 151-160. doi:10.1083/jcb.144.1.151

Sneddon, I. N. (1965). The relation between load and penetration in the axisymmetric boussinesq problem for a punch of arbitrary profile. *Int. J. Eng. Sci.* **3**, 47-57. doi:10.1016/0020-7225(65)90019-4

Spradling, A. C. (1993). Developmental genetics of oogenesis. In *The Development of Drosophila Melanogaster* (ed. M. Bate and A. Martinez Arias), pp. 1-70. New York: Cold Spring Harbor Laboratory Press.

Tran, D. H. and Berg, C. A. (2003). *bullwinkle* and *shark* regulate dorsal-appendage morphogenesis in *Drosophila* oogenesis. *Development* **130**, 6273-6282. doi:10.1242/dev.00854

Urbano, J. M., Torgler, C. N., Molnar, C., Tepass, U., López-Varea, A., Brown, N. H., de Celis, J. F. and Martín-Bermudo, M. D. (2009). *Drosophila* laminins act as key regulators of basement membrane assembly and morphogenesis. *Development* **136**, 4165-4176. doi:10.1242/dev.044263

Viktorinová, I. and Dahmann, C. (2013). Microtubule polarity predicts direction of egg chamber rotation in *Drosophila*. *Curr. Biol.* **23**, 1472-1477. doi:10.1016/j.cub.2013.06.014

Viktorinová, I., König, T., Schlichting, K. and Dahmann, C. (2009). The cadherin Fat2 is required for planar cell polarity in the *Drosophila* ovary. *Development* **136**, 4123-4132. doi:10.1242/dev.039099

Walma, D. A. C. and Yamada, K. M. (2020). The extracellular matrix in development. *Development* **147**, dev175596. doi:10.1242/dev.175596

Wang, X., Li, X., Bank, R. A. and Agrawal, C. M. (2002). Effects of collagen unwinding and cleavage on the mechanical integrity of the collagen network in bone. *Calcif. Tissue Int.* **71**, 186-192. doi:10.1007/s00223-001-1082-2

Wolfstetter, G. and Holz, A. (2012). The role of LamininB2 (LanB2) during mesoderm differentiation in *Drosophila*. *Cell. Mol. Life Sci.* **69**, 267-282. doi:10.1007/s00018-011-0652-3

Wolfstetter, G., Shirinian, M., Stute, C., Grabbe, C., Hummel, T., Baumgartner, S., Palmer, R. H. and Holz, A. (2009). Fusion of circular and longitudinal muscles in *Drosophila* is independent of the endoderm but further visceral muscle differentiation requires a close contact between mesoderm and endoderm. *Mech. Dev.* **126**, 721-736. doi:10.1016/j.mod.2009.05.001

Wu, Y. and Ge, G. (2019). Complexity of type IV Collagens: from network assembly to function. *Biol. Chem.* **400**, 565-574. doi:10.1515/hsz-2018-0317

Yamada, M. and Sekiguchi, K. (2015). Molecular basis of laminin-integrin interactions. *Curr. Top. Membr.* **76**, 197-229. doi:10.1016/bs.ctm.2015.07.002

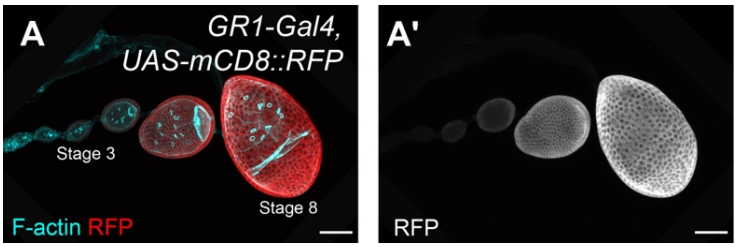

Fig. S1. *GR1-Gal4* activity

(A, A') F-actin (cyan) and RFP (red in A, grey in A') staining of stage 8 *GR1-Gal4, UAS-mCD8::RFP* egg chambers. Scale bars: 50 µm.

.

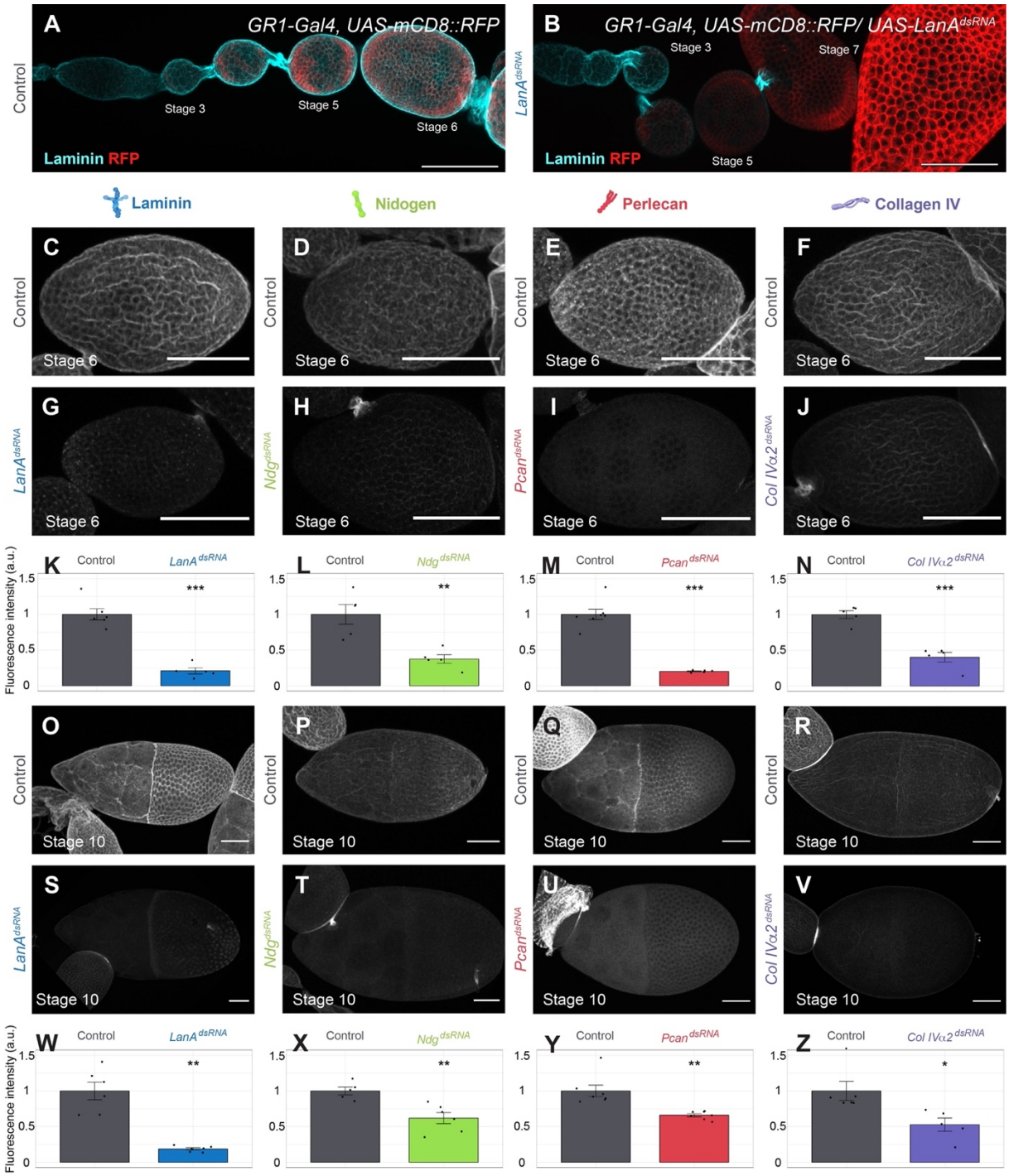

Fig. S2. Knock-down efficiency at stage 6 and 10

(A,B) Ovarioles of the genotype *GR1-Gal4, UAS-mCD8::RFP* as control (A), and *GR1-Gal4* driven *UAS-mCD8::RFP*/*UAS-LanA*^{dsRNA} (B) stained with anti-Laminin (cyan) and anti-RFP (red) antibodies.

(C-J) Stage 6 egg chambers of the genotype *GR1-Gal4* as control (C-F), and *GR1-Gal4* driven *UAS-LanA*^{dsRNA} (G), *UAS-Ndg*^{dsRNA} (H), *UAS-Pcan*^{dsRNA} (I) or *UAS-Col IVα2*^{dsRNA} (J) are shown. Anti-Laminin antibody staining (C,G), anti-Nidogen antibody

staining (D,H), anti-Perlecan antibody staining (E,I) and anti-GFP antibody staining in a *Col IVα2::GFP* genetic background (F,J) are depicted.

(K-N) Mean fluorescence intensity, normalized to controls, of the stainings shown in (C-J). *n*>4 egg chambers per genotype and staining. Mean±sem are shown. ** p<0.005, *** p<0.001 (Welsh two-sided t-test). Black dots show single measurements.

(O-V) Stage 10 egg chambers of the genotype *GR1-Gal4* as control (O-R), and *GR1-Gal4* driven *UAS-LanA*^{dsRNA} (S), *UAS-Ndg*^{dsRNA} (T), *UAS-Pcan*^{dsRNA} (U) or *UAS-Col IVα2*^{dsRNA} (V) are shown. Anti-Laminin antibody staining (O,S), anti-Nidogen antibody staining (P,T), anti-Perlecan antibody staining (Q,U) and anti-GFP antibody staining in a *Col IVα2::GFP* genetic background (R,V) are depicted.

(W-Z) Mean fluorescence intensity, normalized to controls, of the stainings shown in (O-V). *n*>4 egg chambers per genotype and staining. Mean±sem are shown. * p<0.01, ** p<0.005 (Welsh two-sided t-test). Black dots show single measurements.

Scale bars: 50 μm.

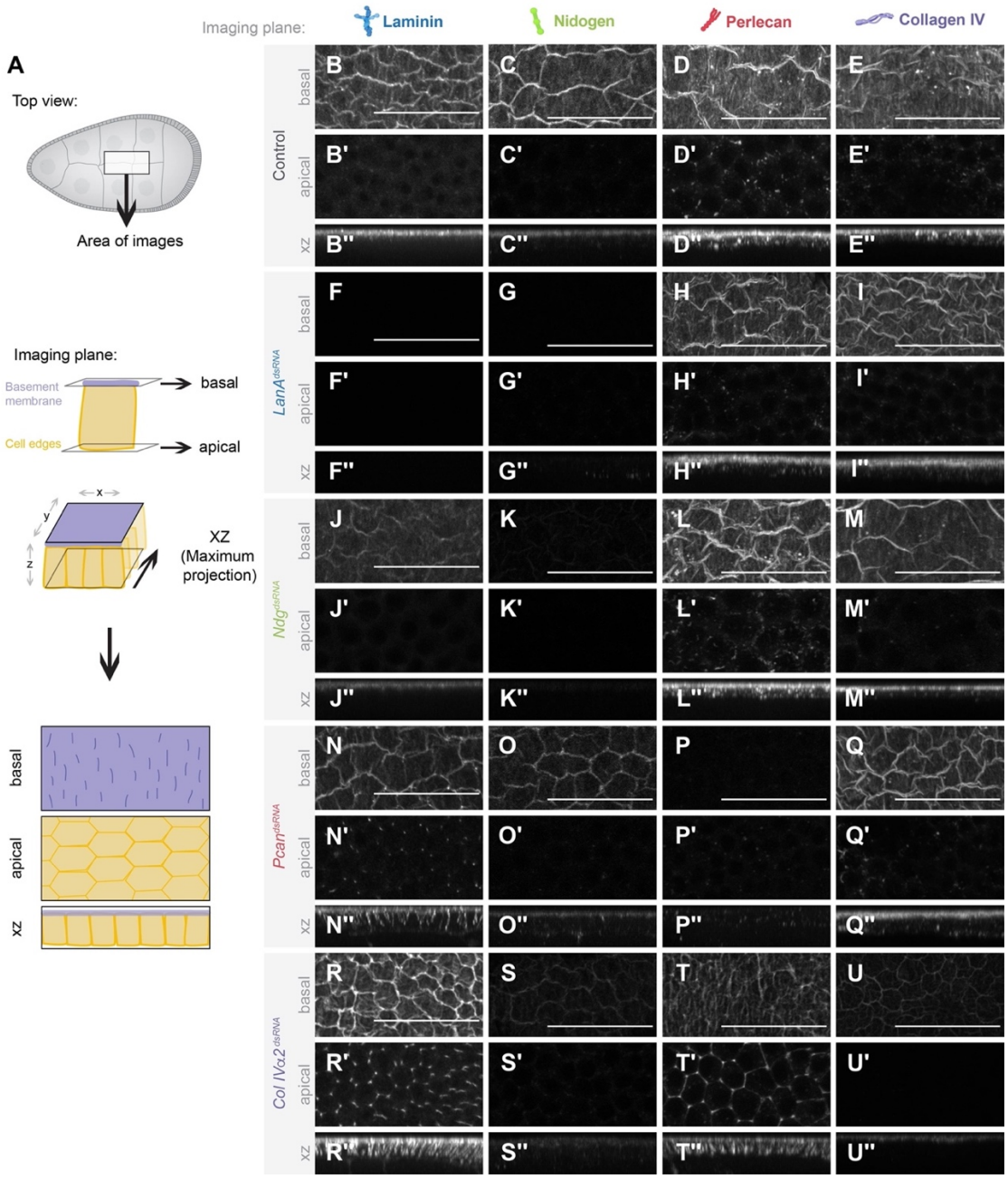

Fig. S3. Subcellular protein localization in knock-downs

(A) Schematic illustration of imaging planes applied in B-U''.

(B-U'') Basal, apical and xz imaging planes from the central region of stage 8 egg chambers of the genotype *GR1-Gal4* as control (B-E''), and *GR1-Gal4* driven *UAS-LanA*^{dsRNA} (F-I''), *UAS-Ndg*^{dsRNA} (J-M''), *UAS-Pcan*^{dsRNA} (N-Q'') or *UAS-Col IVα2*^{dsRNA} (R-U'') are shown. Anti-Laminin antibody staining (B-B'',F-F'',J-J",N-N'',R-R''), anti-Nidogen antibody staining (C-C'',G-G'',K-K",O-O'',S-S''), anti-Perlecan antibody staining (D-D'',H-H'',L-L",P-P'',T-T'') and anti-GFP antibody staining in a *Col IVα2::GFP* genetic background (E-E'',I-I'',M-M",Q-Q'',U-U'') are depicted. Scale bars: 50 µm.

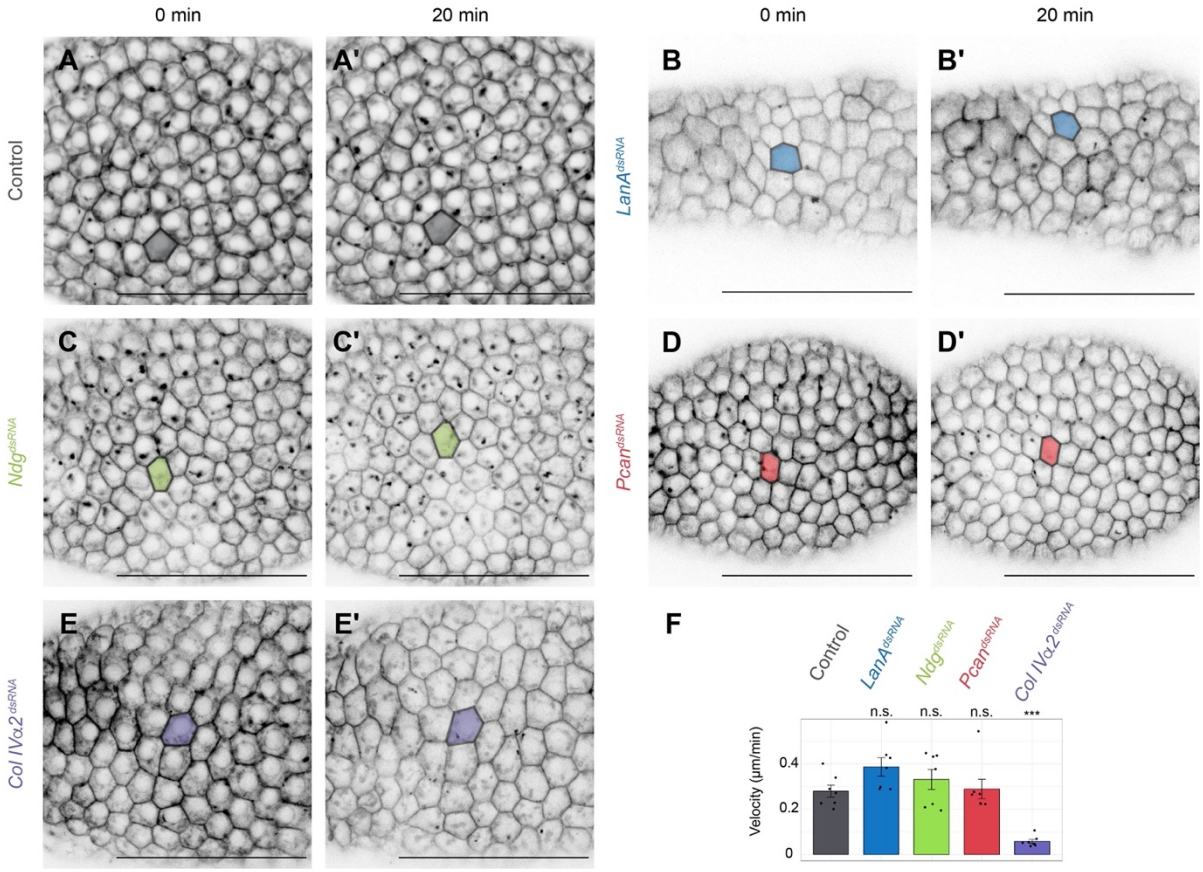

Fig. S4. Egg chamber rotation

(A-E') Time-lapse analysis of *ex vivo* cultured stage 8 egg chambers at 0 min (A,B,C,D,E) and at 20 min (A',B',C',D',E'). *GR1-Gal4, UAS-mCD8::RFP* as control (A,A'), and *GR1-Gal4* driven *UAS-mCD8::RFP/UAS-LanA*^{dsRNA} (B,B'), *UAS-mCD8::RFP/UAS-Ndg*^{dsRNA} (C,C') *UAS-mCD8::RFP/UAS-Pcan*^{dsRNA} (D,D'), *UAS-mCD8::RFP/UAS-ColIVα 2*^{dsRNA} (E,E') are shown. mCD8::RFP fluorescence is shown. A single cell is outlined at 0 min and at 20 min to illustrate the velocity of egg chamber rotation. Scale bars: 50 µm.

(F) Velocity of egg chamber rotation for stage 8 egg chambers of the indicated genotypes. *n*=7 egg chambers per genotype. Mean±sem are shown. n.s. (not significant). *** p<0.001 (Welsh two-sided t-test). Black dots show single measurements.

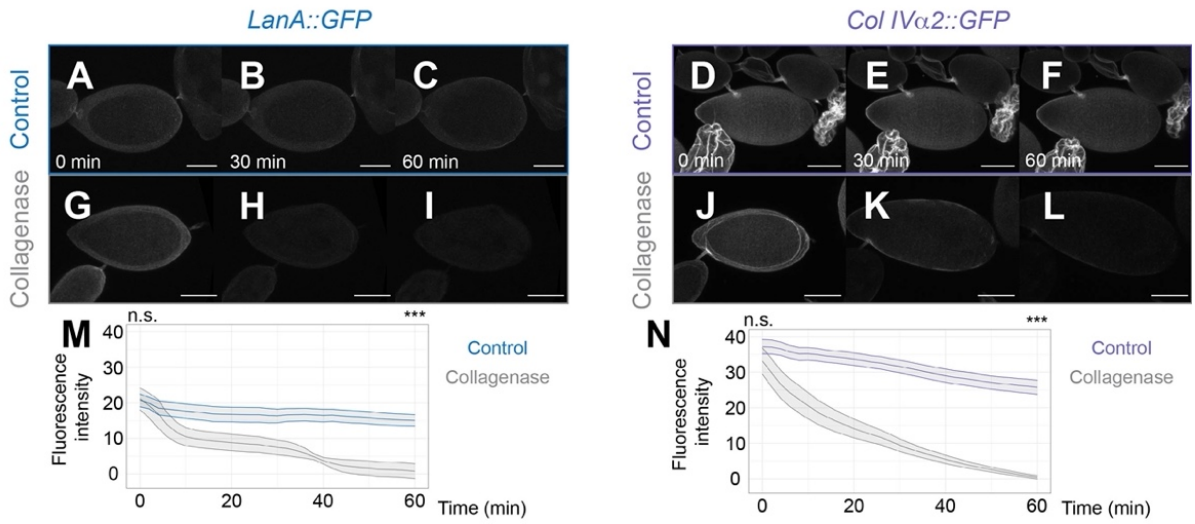

Fig. S5. Collagenase treatment decreases Col IV and Lan A protein levels (A-L) Time series of egg chambers expressing *LanA::GFP* (A-C,G-I) or *Col IVα2::GFP* (D-F,J-L) without treatment (control, A-F) or treated with collagenase at t = 0 min (G-L). Scale bars: 50 µm. **(M,N)** Corrected mean fluorescence intensity (a.u.) of LanA::GFP (M) or Col IVα2::GFP (N) over time for control and collagenase treatment. *n*=5 egg chambers. Mean±sem are shown. At 0 min: n.s. (not significant); at 60 min. *** p<0.001 (Welsh two-sided t-test).